THE JOURNAL OF BIOLOGICAL CHEMISTRY VOL. 285, NO. 29, pp. 22639–22650, July 16, 2010

Multifunctional Nanoparticles Delivering Small Interfering RNA and Doxorubicin Overcome Drug Resistance in Cancer*[S]

Received for publication, March 23, 2010, and in revised form, May 5, 2010 Published, JBC Papers in Press, May 11, 2010, DOI 10.1074/jbc.M110.125906

Yunching Chen[1], **Surendar Reddy Bathula, Jun Li, and Leaf Huang**

From the Division of Molecular Pharmaceutics, Eshelman School of Pharmacy, University of North Carolina at Chapel Hill, Chapel Hill, North Carolina 27599

Drug resistance is a major challenge to the effective treatment of cancer. We have developed two nanoparticle formulations, cationic liposome-polycation-DNA (LPD) and anionic liposome-polycation-DNA (LPD-II), for systemic co-delivery of doxorubicin (Dox) and a therapeutic small interfering RNA (siRNA) to multiple drug resistance (MDR) tumors. In this study, we have provided four strategies to overcome drug resistance. First, we formed the LPD nanoparticles with a guanidinium-containing cationic lipid, *i.e. N*,*N*-distearyl-*N*-methyl-*N*-2-(*N*′-arginyl) aminoethyl ammonium chloride, which can induce reactive oxygen species, down-regulate MDR transporter expression, and increase Dox uptake. Second, to block angiogenesis and increase drug penetration, we have further formulated LPD nanoparticles to co-deliver vascular endothelial growth factor siRNA and Dox. An enhanced Dox uptake and a therapeutic effect were observed when combined with vascular endothelial growth factor siRNA in the nanoparticles. Third, to avoid P-glycoprotein-mediated drug efflux, we further designed another delivery vehicle, LPD-II, which showed much higher entrapment efficiency of Dox than LPD. Finally, we delivered a therapeutic siRNA to inhibit MDR transporter. We demonstrated the first evidence of c-Myc siRNA delivered by the LPD-II nanoparticles down-regulating MDR expression and increasing Dox uptake *in vivo*. Three daily intravenous injections of therapeutic siRNA and Dox (1.2 mg/kg) co-formulated in either LPD or LPD-II nanoparticles showed a significant improvement in tumor growth inhibition. This study highlights a potential clinical use for the multifunctional nanoparticles with an effective delivery property and a function to overcome drug resistance in cancer. The activity and the toxicity of LPD- and LPD-II-mediated therapy are compared.

The occurrence of drug resistance is a main impediment to the success of cancer chemotherapy. Cancer cells develop different ways to be resistant to chemotherapy drugs. Overexpression of drug transporter proteins, such as P-glycoprotein (P-gp)[2] plays a key role in regulating drug resistance. Development of strategies to down-regulate the expression of P-gp or inhibit P-gp function has been the major subject of cancer research. For example, one of the strategies to overcome MDR is to use carriers like nanoparticles to avoid P-gp-mediated drug efflux. Only the drug presenting in the cell membrane can be effluxed out of the cancer cell. The drug delivered by nanoparticles is internalized in the cytoplasm or the lysosome and not pumped out by P-gp (1). Dox-loaded liposomes are able to overcome MDR by increasing Dox uptake in the nuclei and extending retention in the nuclei of the MDR cells (2, 3).

Small interfering RNA (siRNA) is a promising novel approach of cancer therapy. It offers a new strategy to down-regulate the targeted oncogene for therapeutic intervention. Systemically delivering siRNA to tumors remains a major hurdle in cancer gene therapy (4, 5). Major problems of siRNA delivery include poor cellular uptake, low stability, and rapid clearance from the systemic circulation. We have developed a cationic lipid containing both a guanidinium and a lysine residue as a cationic head group that can down-regulate mitogen-activated protein kinase (MAPK) signaling, form cationic liposome-polycation-DNA (LPD) to intravenously deliver siRNA to the solid tumor in high efficiency, and achieve a synergistic therapeutic effect with siRNA on a human lung cancer model (6). In this study, we further explored the biological activity of the guanidinium-containing cationic lipid, *i.e. N*,*N*-distearyl-*N*-methyl-*N*-2-(*N*′-arginyl) aminoethyl ammonium chloride (DSAA), which may play a role in overcoming drug resistance in tumors. However, nanoparticles containing cationic lipid such as DSAA showed a poor entrapment efficiency of Dox and induced immunotoxicity in mice.

To combat these problems, we have further developed the multifunctional LPD-II nanoparticles made with anionic lipids that co-deliver siRNA and Dox into the MDR tumor cells and trigger a synergistic anti-cancer effect. We co-formulated siRNA and Dox in the LPD-II nanoparticles via Dox intercalation into the DNA in the nanoparticles. Both LPD and LPD-II nanoparticles were targeted specifically to the tumor cells by modification with anisamide (AA), a ligand of sigma receptor

* This work was supported, in whole or in part, by National Institutes of Health Grant CA129825.

[S] The on-line version of this article (available at http://www.jbc.org) contains supplemental Table S1 and Figs. S1–S4.

[1] To whom correspondence should be addressed: 1319 Kerr Hall, University of North Carolina at Chapel Hill, Chapel Hill, NC 27599. Tel.: 919-843-4704; Fax: 919-966-0197; E-mail: yunching@email.unc.edu.

[2] The abbreviations used are: P-gp, P-glycoprotein; LPD, cationic liposome-polycation-DNA; LPD-II, anionic liposome-polycation-DNA; PEG, polyethylene glycol; Dox, doxorubicin; siRNA, small interfering RNA; AA, anisamide; MDR, multiple drug resistance; ROS, reactive oxygen species; VEGF, vascular endothelial growth factor; DSAA, *N*,*N*-distearyl-*N*-methyl-*N*-2-(*N*′-arginyl) aminoethyl ammonium chloride; DOTAP, 1,2-di-(9Z-octadecenoyl)-3-trimethylammonium-propane; DOPA, 1,2-di-(9Z-octadecenoyl)-*sn*-glycero-3-phosphate; DCFH-DA, 2′,7′-dichlorodihydrofluorescein diacetate; TEM, transmission electron microscopy; TUNEL, TdT dUTP nick end labeling; FITC, fluorescein isothiocyanate; Boc, *t*-butoxycarbonyl; PBS, phosphate-buffered saline; AM, acetoxymethylester; DAPI, 4′,6-diamidino-2-phenylindole; IL, interleukin; MFI, mean fluorescence intensity.

overexpressed in many human cancer cells. Two different siRNAs, VEGF and c-Myc siRNAs, are selected in this study to achieve the enhanced drug uptake and anti-cancer effect. We hypothesized that therapeutic siRNAs delivered to the MDR cells will down-regulate the target genes and sensitize the tumor cells to the co-delivered Dox, resulting in an enhanced therapeutic activity of the nanomedicine. The experiments were carried out in a xenograft model of the NCI/ADR-RES tumor.

EXPERIMENTAL PROCEDURES

Materials—DOPA, 1,2-dioleoyl-*sn*-glycero-3-phosphoethanolamine, and cholesterol were purchased from Avanti Polar Lipids, Inc. (Alabaster, AL). Protamine sulfate (fraction X from salmon) and calf thymus DNA were purchased from Sigma-Aldrich (St. Louis, MO). Dox was purchased from IFFECT CHEMPHAR (Hong Kong). Synthetic 19-nucleotide RNAs with 3′-UU overhangs on both sequences were purchased from Dharmacon (Lafayette, CO). For quantitative studies, FITC or cy5.5 was conjugated to 5′ sense sequence. 5′-cy5.5- and 5′-FITC-labeled siRNA sequences were also obtained from Dharmacon. The sequence of c-Myc siRNA was 5′-AACGUUAGCUUCACCAACAUU-3′, and the VEGF siRNA was 5′-GCAGAAUCAUCACGAAGUG-3′. The sequence of control siRNA with sequence 5′-AATTCTCCGAACGTGTCACGT-3′ was obtained from Dharmacon.

Synthesis of DSAA—DSAA is a nonglycerol-based guanidine head group containing cationic lipid synthesized in five steps. *N*-Alkylation by *n*-octadecyl bromide and subsequent Boc deprotection of mono-Boc-protected ethylene diamine yielded the mixed primary tertiary amine N^1,N^1-dioctadecylethane-1,2-diamine. Tri-*N*-tert-butoxycarbonyl protected arginine conjugation to the primary amine group by the conventional 1-ethyl-3-(3-dimethylaminopropyl)carbodiimide. Quaternization of the tertiary amine group using methyl iodide on the above obtained product gave tri-*N*-tert-butoxycarbonyl-protected DSAA. To obtain the final product DSAA, Boc group deprotection with trifluoroacetic acid and chloride ion exchange with Amberlyst A 27(Cl^-) ion exchange resin were carried out. The resulting compound was characterized by using ^{1}H NMR spectra and liquid secondary ion mass spectrometry. Detailed synthetic procedures and spectral and purity data will be delineated elsewhere.[3]

Cell Culture—NCI/ADR-RES and OVCAR-8 cells were a kind gift from Dr. Russell Mumper (University of North Carolina School of Pharmacy). NCI-ADR/RES is a multidrug-resistant ovarian cancer cell line derived from OVCAR-8 cells (drug-sensitive line) in a poorly documented manner (NCI, National Institutes of Health web site). NCI/ADR-RES cells were maintained in Dulbecco's modified Eagle's medium high glucose with GlutaMAX (Invitrogen, Carlsbad, CA) supplemented with 10% fetal bovine serum (Invitrogen), 100 units/ml penicillin, and 100 μg/ml streptomycin (Invitrogen).

Experimental Animals and Tumor Model—Female athymic nude mice 6–8 weeks of age were purchased from the National Cancer Institute, Frederick, National Institutes of Health. The mice were injected subcutaneously in the right flank with 5×10^6 NCI/ADR-RES cells in 0.1 ml of PBS. All of the work performed on animals was in accordance with and permitted by the University of North Carolina Institutional Animal Care and Use Committee.

Functional Expression of P-gp—Calcein-AM has been used as a functional probe for the detection of P-gp activity (7). The cells were treated with lipids and incubated with 1 μmol/liter of calcein-AM for 15 min at 37 °C in Dulbecco's modified Eagle's medium. The cells were resuspended in calcein-AM-free medium, washed twice in PBS, and analyzed using flow cytometry. The uptake calcein-AM in the cells was expressed as: folds of untreated = $(MFI_{treatment} - MFI_{unstained})/(MFI_{untreated} - MFI_{unstained})$.

Analysis of ROS—NCI/ADR-RES cells (1×10^6/well) were seeded into 12-well plates. The cells were treated with lipids in serum-containing medium at 37 °C. Then the cells were incubated with 20 μM DCFH-DA (Sigma-Aldrich) in serum-containing medium for 30 min at 37 °C. The cells were quickly washed and immediately analyzed by flow cytometry.

Preparation of Nanoparticle Formulations—LPD nanoparticles were prepared according to the previously described method with slight modifications (8). Briefly, cationic liposomes composed of cholesterol and DOTAP or DSAA (1:1 molar ratio) were prepared by thin film hydration followed by membrane extrusion to reduce the particle size. 15 μl of protamine (2 mg/ml), 140 μl of deionized water, and 24 μl of a mixture of siRNA and calf thymus DNA (2 mg/ml) were mixed and kept at room temperature for 10 min before adding 120 μl of cationic liposome (20 mM). The formulations stand at room temperature for 10 min before the addition of DSPE-PEG. The formulations were then mixed with 70 μl of DSPE-PEG or DSPE-PEG-AA (10 mg/ml) and kept at 50–60 °C for 10 min for the attachment of the PEG chains to the surface membrane of the nanoparticles.

Preparation of PEGylated LPD-II Formulations—LPD-II was prepared according to the previously described method with slight modifications (9). Briefly, anionic liposomes composed of DOPA, 1,2-dioleoyl-*sn*-glycero-3-phosphoethanolamine, and cholesterol (2:1:1 molar ratio) were prepared by thin film hydration followed by membrane extrusion to reduce the particle size. To prepare LPD-II, 48 μl of protamine (2 mg/ml), 60 μl of deionized water, and 24 μl of a mixture of siRNA and calf thymus DNA (2 mg/ml) were mixed and kept at room temperature for 10 min before adding 90 μl of anionic liposome (20 mM). LPD-II was left at room temperature for 10 min before the addition of DSPE-PEG. It was then mixed with 54 μl of DSPE-PEG or DSPE-PEG-AA (10 mg/ml) and kept at 50–60 °C for 10 min for the attachment of the PEG chains to the surface membrane of the nanoparticles.

Transmission Electron Microscopy (TEM) Image—TEM images of the LPD-II nanoparticles were acquired by the use of JEOL 100CX II TEM (JEOL, Japan). Briefly, 5 μl of LPD-II nanoparticles was dropped on to a 300 mesh carbon coated copper grid (Ted Pella, Inc., Redding, CA). Excess sample was removed by blotting with a filter paper. The grid was air-dried and viewed in TEM without staining. The scale bar was automatically shown in the image according to the magnification.

[3] S. R. Bathula, Y. Chen, and L. Huang, unpublished observations.

Cellular Uptake Study—NCI/ADR-RES cells (1×10^5/well) were seeded in 12-well plates (Corning Inc., Corning, NY) 12 h before experiments. The cells were treated with different formulations at a concentration of 250 nM for 5′-FITC-labeled siRNA or 1.5 μM Dox in serum-containing medium at 37 °C for 4 h. The cells were washed twice with PBS, counterstained with DAPI, and imaged using a Leica SP2 confocal microscope. Dox and siRNA uptake of NCI/ADR-RES cells was also measured by flow cytometry. Briefly, the cells were treated with different formulations at a concentration of 250 nM 5′-FITC-labeled siRNA or 1.5 μM Dox in serum-containing medium at 37 °C for 1 h. The cells were harvested and resuspended at a concentration of 1×10^6 cells/ml. The cells were washed with PBS and analyzed for fluorescence by flow cytometry.

Gene Silencing Study—NCI/ADR-RES tumor-bearing mice (tumor size, ~1 cm^2) were intravenously injected with siRNA and Dox in different formulations (1.2 mg of siRNA/kg, one injection/day for 2 days). A day after the third injection, the tumors were collected, paraffin-embedded, and sectioned. 7.25-μm-thick sections were immunostained with primary antibodies and visualized by using kits from DakoCytomation. The samples were imaged by using a Nikon Microphot SA microscope or Leica SP2 confocal microscope.

Quantitative Reverse Transcription-PCR—NCI/ADR-RES tumor-bearing mice (tumor size, ~1 cm^2) were intravenously injected with siRNA and Dox in different formulations (1.2 mg of siRNA/kg, one injection/day for 2 days). A day after the third injection, the mice were killed, and tumor samples were collected. Total RNA were extracted with the RNeasy® mini kit (Qiagen, Valencia, CA) by following the manufacturer's protocol. cDNA was then prepared in the presence of reverse transcriptase (Promega, Madison, WI). The mRNA levels were determined by an ABI PRISM HT7500 sequence detection system (Applied Biosystems, Foster City, CA) as described previously (10). The oligomer pairs used for the amplification of PCR products were AAGCCACAGCATACATCC (forward primer for c-Myc), TTACGCACAAGAGTTCCG (reverse primer for c-Myc), CACCACCAACTACTTAGC (forward primer for glyceraldehyde-3-phosphate dehydrogenase), and GTAGAGGCAGGAATGATG (reverse primer for glyceraldehyde-3-phosphate dehydrogenase).

Western Blot Analysis—NCI/ADR-RES tumor-bearing mice (tumor size, ~1 cm^2) were intravenously injected with siRNA and Dox in different formulations (1.2 mg of siRNA/kg, one injection/day for 2 days). A day after the third injection, the mice were killed, and the tumor samples were collected. Total protein (40 μg) isolated from the tumors was loaded on a polyacrylamide gel. Tumor lysates were separated on a 10% acrylamide gel and transferred to a polyvinylidene difluoride membrane. The membranes were blocked for 1 h in 5% skim milk and then incubated with polyclonal antibody against c-Myc (Santa Cruz Biotechnology, Inc., Santa Cruz, CA) overnight. The membranes were washed in PBST (PBS with 0.1% Tween 20) three times and then incubated for 1 h with the secondary antibody. The membranes were washed four times and then developed by an enhanced chemiluminescence system according to the manufacturer's instructions (PerkinElmer Life Sciences, Waltham, MA). The intensity of the bands was quantified by Photoshop histogram.

Tumor Uptake Study—Mice with a tumor size of ~1 cm^2 were intravenously injected with cy5.5-labeled siRNA (1.2 mg/kg) and Dox (1.2 mg/kg) in different formulations. 4 h later, the mice were killed, and the tissues were collected, fixed in 10% formalin, and embedded in paraffin. The tumor tissues were sectioned (7.25 μm thick) and imaged using a Leica SP2 confocal microscope.

TdT dUTP Nick End Labeling (TUNEL) Assay—TUNEL staining was performed as recommended by the manufacturer's protocol (Promega, Madison, WI). NCI/ADR-RES tumor-bearing mice were given intravenous injections of the siRNA and Dox formulated in the nanoparticles. 24 h after the second injection, the mice were sacrificed, and the tumors were collected for TUNEL staining. Images from TUNEL-stained tumor sections were captured with Nikon ECLIPSE Ti-U microscopy.

Tumor Growth Inhibition Study—NCI/ADR-RES tumor-bearing mice (size, 16–25 mm^2) were intravenously injected with different formulations containing siRNA (1.2 mg/kg) or Dox (1.2 mg/kg) once/day for 3 days. Tumor size in the treated mice was measured after treatment.

Statistical Analysis—All of the statistical analyses were performed by Student's *t* test. The data were considered statistically significant when the *p* value was less than 0.05.

RESULTS

DSAA, a Guanidinium-containing Lipid, Serves as a P-gp Inhibitor and a Carrier of siRNA and Dox—Our first strategy is to use a cationic lipid as a P-gp inhibitor as well as a drug carrier. To determine whether the cationic lipid containing a guanidinium residue overcomes MDR, we first studied the uptake of Dox in NCI/ADR-RES cells. NCI/ADR-RES cells were treated with different lipids for different doses. Then cells were treated with the indicated concentration of free Dox. The structures of different lipids used in this study were illustrated in Fig. 1*A*. As shown in Fig. 1*B*, incubation with DSAA resulted in a substantial increase in Dox accumulation. The lipids without guanidine groups only caused a slight increase in Dox uptake. Besides, we also evaluated the ability of different lipids to inhibit P-gp using the calcein-AM assay in the resistant and sensitive cell lines (Fig. 1*C* and supplemental Fig. S1). In drug-resistant NCI/ADR-RES cells, the fluorescence generated from intracellular calcein significantly increased in a dose-dependent manner when cells were treated with DSAA. In contrast, DOTAP or the lipids without guanidinium groups only caused a slight increase in intracellular calcein fluorescence. However, intracellular calcein fluorescence remained only slightly changed after treatment with 10 or 50 μM DSAA for 1 h in the drug-sensitive OVCAR-8 cells (supplemental Fig. S1).

Because drug-resistant cells treated with DSAA resulted in significantly enhanced Dox uptake and inhibition of P-gp activity, we further studied the biological functions of DSAA in some detail. The guanidinium head group of DSAA may induce ROS, which down-regulates P-gp expression in MDR cells (11, 12). To address this hypothesis, NCI/ADR-RES cells were treated with DSAA or DOTAP at different doses and further incubated

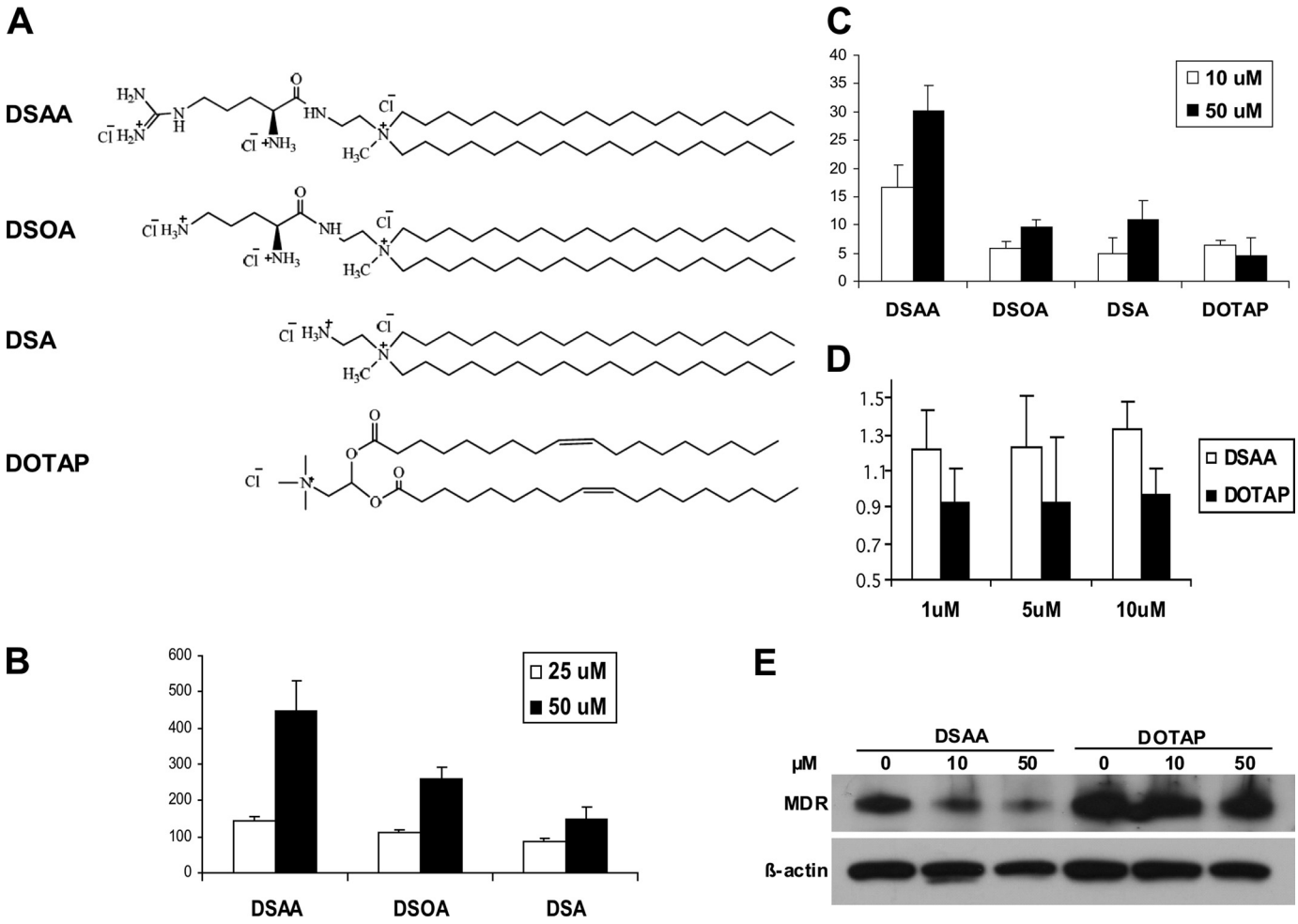

FIGURE 1. **Treatment of DSAA-enhanced Dox uptake in NCI/ADR-RES cells by down-regulating MDR expression and activity.** *A*, chemical structures of cationic lipids. *B*, quantitative measurement of Dox uptake after 1 h of incubation with different concentrations of cationic lipids by flow cytometry. *C*, quantitative measurement of calcein-AM uptake after 1 h of incubation with different concentrations of cationic lipids by flow cytometry. *D*, ROS generation by DSAA or DOTAP after 1 h of incubation with different concentrations of DSAA or DOTAP. The ROS content of cells was analyzed by flow cytometry; $n = 3$. *E*, MDR expression in NCI/ADR-RES cells after incubation with 10 or 50 μM DSAA and DOTAP for 24 h. *DSA*, *N*-methyl-*N*,*N*-distearyl ammonium chlolride.

with DCFH-DA. The cellular ROS content was detected by using flow cytometry. As shown in Fig. 1*D*, DSAA could significantly generate ROS in NCI/ADR-RES cells 1 h after treatment. However, the cellular ROS content remained unchanged after treatment with 1, 5, or 10 μM DOTAP for 1 h. Furthermore, MDR expression in MDR cells was significantly suppressed after treatment with 10 or 50 μM DSAA (77 and 73% of untreated control, respectively) (Fig. 1*E*). These results suggest that ROS induced by DSAA may reverse drug resistance in NCI/ADR-RES cells by suppressing MDR transporter expression and activity.

Based on the property of DSAA to enhance Dox uptake in the MDR cells, we further used DSAA as a carrier lipid to deliver Dox and siRNA into NCI/ADR-RES cells. We used AA-targeted LPD nanoparticles containing DSAA to specifically deliver Dox and siRNA to the NCI/ADR-RES cells, which express the sigma receptor (data not shown). As shown in supplemental Fig. S2, *A* and *B*), targeted nanoparticles containing DSAA increased both cellular internalization and nuclear uptake of Dox compared with free Dox. The nanoparticles containing DSAA delivered Dox into the cytoplasm of NCI/ADR-RES cells more efficiently than those containing DOTAP. Furthermore, Dox uptake of the cells treated with the targeted nanoparticles was much more than that of cells treated with the nontargeted nanoparticles. Pretreatment or co-incubation of cells with blank-targeted nanoparticles also showed slightly enhanced Dox uptake compared with free Dox. To eliminate the possibility that Dox uptake enhancement was due to apoptosis caused by DSAA, the cells were co-incubated with the caspase-3 inhibitor DEVD-CHO32 and Dox in the targeted nanoparticles containing DSAA. In this treatment, the uptake of Dox was as much as the treatment without the caspase-3 inhibitor (supplemental Fig. S2*A*). The uptake of Dox in the targeted nanoparticles containing DSAA was further examined in the other drug-resistant cells, H460/RES cells, which also overexpress P-gp. As shown in supplemental Fig. S3, targeted nanoparticles containing DSAA increased Dox uptake compared with free Dox in H460/RES cells.

To confirm the ability of DSAA to deliver both Dox and siRNA into NCI/ADR-RES cells, Dox and fluorescently labeled siRNA were co-formulated into different formulations. As shown in Fig. 2*A*, the uptake of Dox and fluorescently labeled

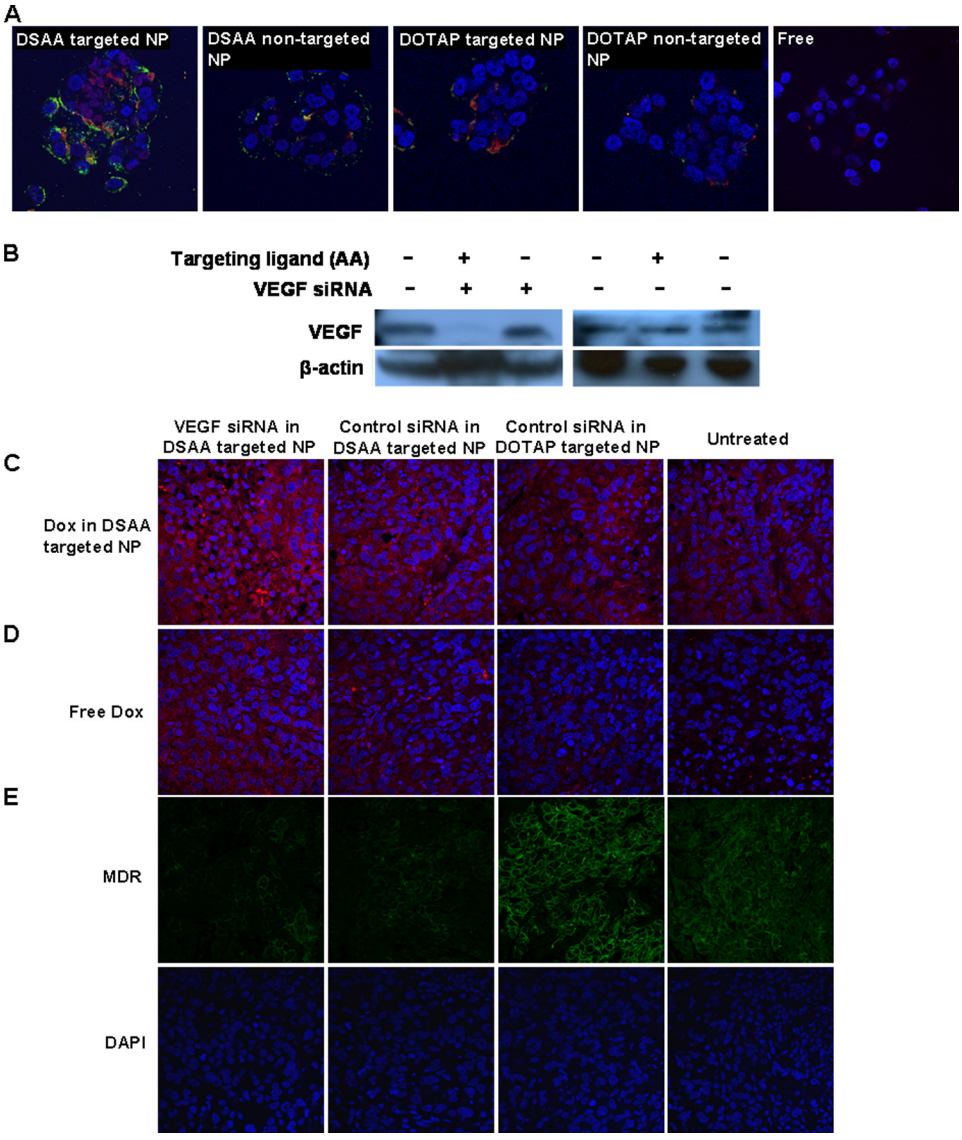

FIGURE 2. **Intracellular uptake of Dox and siRNA and gene silencing effect in NCI/ADR-RES cells *in vitro* and *in vivo*.** *A*, cells were treated with different formulations containing Dox (*red*) and siRNA (*green*) for 2 h and observed by confocal microscopy. The nuclei are *blue* (DAPI). *B*, examination of VEGF expression in NCI/ADR-RES xenograft tumor using Western blot analysis after treatment with different formulations. *C* and *D*, Dox formulated in the targeted nanoparticles containing DSAA (*C*) or free Dox (*D*) was intravenously injected into the tumor-bearing mice 24 h after the second administration of VEGF or control siRNA in the nanoparticles containing DSAA or DOTAP. Tumor uptake of Dox in the targeted nanoparticles containing DSAA (*C*) or free Dox (*D*) 4 h after intravenous administration was observed by confocal microscopy. *E*, MDR expression (*green*) in NCI/ADR-RES tumors 24 h after intravenous administrations of different formulations. NCI/ADR-RES tumor-bearing mice were injected two daily administrations of VEGF or control siRNA (1.2 mg/kg) formulated in the targeted nanoparticles containing DSAA or DOTAP. *NP*, nanoparticles.

siRNA was much greater in cells treated with the formulation prepared with DSAA than the formulation prepared with DOTAP, and the uptake was ligand-dependent. Some Dox co-localized with siRNA in the cytoplasm, and some translocated to the nucleus after treatment of Dox and FITC-siRNA formulated in the targeted nanoparticles containing DSAA. The results indicate that the nanoparticles containing DSAA efficiently co-delivered siRNA and Dox to the NCI/ADR-RES cells, and the delivery was ligand-specific and formulation lipid-dependent.

VEGF siRNA Delivered by Nanoparticles Containing DSAA Showed Significant Gene Silencing and Enhanced Penetration of Drugs in NCI/ADR-RES Tumor—Our second strategy is to use a therapeutic siRNA to inhibit angiogenesis and sensitize the drug-resistant cells to chemotherapy drugs. To examine the biological activities of siRNA co-formulated with Dox in different formulations *in vivo*, the VEGF levels in the subcutaneous NCI/ADR-RES tumor were detected by Western blotting 24 h after two daily intravenous injections of VEGF siRNA and Dox in different formulations (Fig. 2*B*). VEGF expression of the NCI/ADR-RES tumor treated with VEGF siRNA and Dox-containing targeted nanoparticles was significantly suppressed (45% of untreated control) (Fig. 2*B*), whereas VEGF siRNA and Dox-containing nontargeted nanoparticles and a control siRNA and Dox-containing targeted nanoparticles showed no silencing effect. The results indicate that the nanoparticles containing DSAA could systemically deliver siRNA into the tumor tissue and silence the target protein. Furthermore, the silencing effect was specifically controlled by the targeting ligand.

To further study the effect of VEGF siRNA and DSAA on Dox uptake *in vivo*, tumor-bearing mice were given two daily injections of VEGF siRNA or a control siRNA (1.2 mg/kg) formulated in the targeted nanoparticles containing DSAA or DOTAP. 24 h after the second treatment, free Dox or Dox formulated in the targeted nanoparticles containing DSAA was intravenously injected into tumor-bearing mice. The Dox uptake of NCI/ADR-RES tumor tissue in the tumor-bearing mice was observed 4 h after intravenous injections using confocal microscopy. As shown in Fig. 2*D*, Dox formulated in the targeted nanoparticles showed enhanced cytosolic delivery in NCI/ADR-RES cells compared with free Dox. Free Dox uptake was higher in the tumor tissues collected from the mice treated with a control siRNA formulated in the DSAA-containing targeted nanoparticles than in those from the mice treated with a control siRNA formulated in the DOTAP-containing targeted nanoparticles. Furthermore, the formulated Dox uptake also increased in the tumor tissues collected from mice treated with a control siRNA in the DSAA-containing targeted nanoparticles rather than those treated with a control siRNA in the DOTAP-containing targeted nanoparticles (Fig. 2*C*). These results indicate

that DSAA reverses drug resistance in NCI/ADR-RES tumors.

VEGF inhibitors such as bevacizumab can enhance the permeability of the tumor vasculature, which leads to improved penetration of the free or liposome-encapsulated chemotherapy agents in the tumor (13). We hypothesized that VEGF siRNA may improve the penetration and uptake of free Dox or formulated Dox in the drug-resistant tumor. As shown in Fig. 2*D*, free Dox uptake was higher in the tumor tissues collected from the mice treated with VEGF siRNA formulated in the DSAA-containing targeted nanoparticles than in those from the mice treated with a control siRNA formulated in the DSAA-containing targeted nanoparticles. Similarly, the formulated Dox uptake was also enhanced in the tumor tissues collected from mice treated with VEGF siRNA in the targeted nanoparticles compared with those treated with a control siRNA in the targeted nanoparticles (Fig. 2*C*). These results indicate that the uptakes of both free and formulated Dox increased after treatment with VEGF siRNA.

To verify the regulatory effects of DSAA and VEGF siRNA on the expression of MDR transporters *in vivo*, MDR expression in the drug-resistant tumor was examined by immunostaining 24 h after two daily intravenous injections of VEGF siRNA or a control siRNA in different formulations (Fig. 2*E*). MDR expression of the NCI/ADR-RES tumor treated with VEGF siRNA or a control siRNA in the targeted nanoparticles containing DSAA was partially suppressed (Fig. 2*E*). A control siRNA delivered by the targeted nanoparticles containing DOTAP showed no effect. Thus, the data indicate that inhibition of the MDR expression mediated by the targeted nanoparticles was formulation lipid-dependent but not siRNA sequence-specific. Taken together, these results demonstrate a combination effect between VEGF siRNA and DSAA in promoting Dox uptake in NCI/ADR-RES tumors. A combination effect between VEGF siRNA and DSAA in promoting cellular apoptosis and tumor growth inhibition was further tested.

VEGF siRNA and Dox Co-delivered by Nanoparticles Containing DSAA Showed Significant Therapeutic Effect in NCI/ADR-RES Tumor—To examine the therapeutic activities of siRNA and Dox in the different formulations, we stained for the apoptotic markers in NCI/ADR-RES tumors (Fig. 3*A*). Fig. 3*A* indicates that ~8% of NCI/ADR-RES cells treated with VEGF siRNA and Dox in the targeted nanoparticles containing DSAA underwent apoptosis as detected by the TUNEL staining. This value was significantly higher than the cells treated with control siRNA formulated in the targeted nanoparticles containing DSAA or VEGF or control siRNA formulated in the targeted nanoparticles containing DOTAP. To further elucidate the therapeutic effects of Dox and VEGF siRNA in the nanoparticles containing DSAA, tumor growth inhibitory effects were evaluated after treatments of different formulations. Three injections of VEGF siRNA alone in the targeted nanoparticles containing DSAA showed a partial inhibition of tumor growth ($p < 0.05$ comparing with the untreated control at day 18) (Fig. 3*B*). Free Dox had no therapeutic effect. A synergistic tumor growth inhibition was observed when mice were treated with Dox and VEGF siRNA co-formulated in the targeted nanoparticles containing DSAA. Thus, targeted nanoparticles loaded

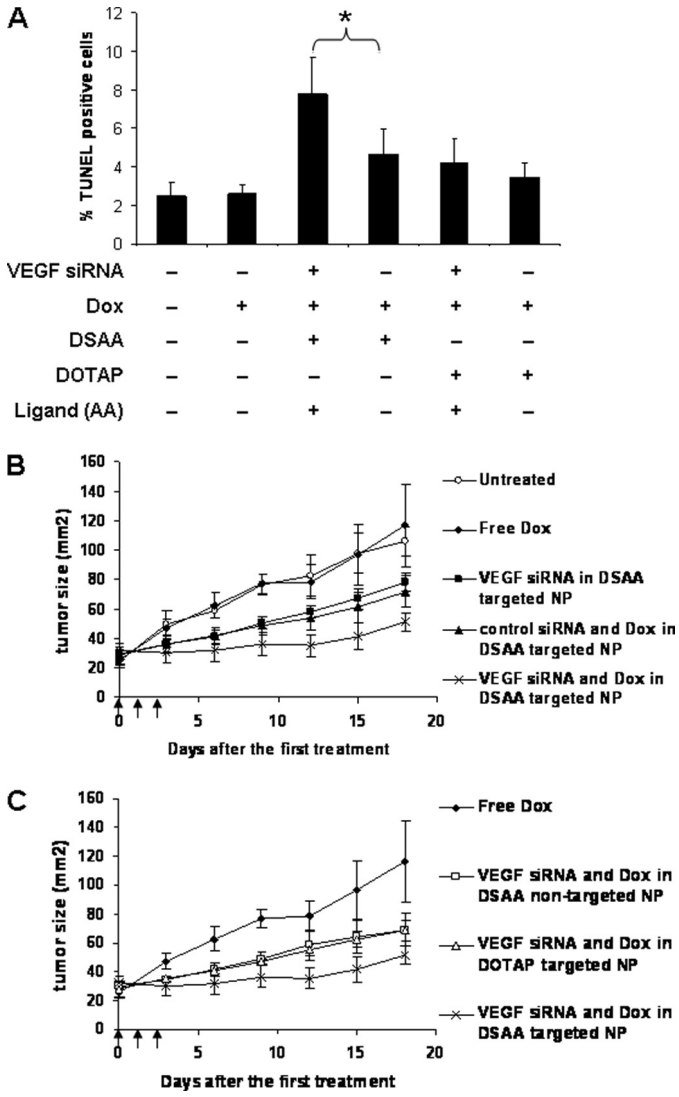

FIGURE 3. **Apoptosis induction and growth inhibition in NCI/ADR-RES xenograft tumor.** *A*, quantitative analysis of TUNEL positive staining in the NCI/ADR-RES tumors collected after three daily intravenous administrations of siRNA (1.2 mg/kg) and Dox (1.2 mg/kg) in different formulations; $n = 3–6$. The *asterisk* indicates $p < 0.05$. *B*, comparison of therapeutic efficacy of VEGF and control siRNAs co-formulated with Dox in the targeted nanoparticles containing DSAA. *C*, comparison of therapeutic efficacy of the targeted and nontargeted nanoparticles containing DSAA or DOTAP. The *arrows* indicate the intravenous administrations of siRNA (1.2 mg/kg) and Dox (1.2 mg/kg). The data are the mean values; $n = 4–5$.

with both VEGF siRNA and DSAA could sensitize MDR cells to co-formulated Dox. Furthermore, VEGF siRNA and Dox in the targeted nanoparticles containing DOTAP or in the nontargeted nanoparticles containing DSAA showed less therapeutic effect compared with the treatment of VEGF siRNA and Dox in the targeted nanoparticles containing DSAA (Fig. 3*C*). The results indicate that the therapeutic effects of the formulations are both lipid- and ligand-dependent. Taken together, DSAA-containing targeted nanoparticles loaded with both Dox and VEGF siRNA could overcome P-gp-mediated drug resistance. All therapeutic agents in a single formulation worked together to induce apoptosis and suppress tumor growth by inhibiting the mechanisms involved in drug resistance and survival.

However, cationic lipids such as DSAA competed with Dox for interacting with DNA, resulting in a low entrapment effi-

ciency of Dox in the nanoparticles (14). The amount of Dox loaded into the final formulation was only ~10% of the total Dox determined by Sepharose CL 2B column chromatography. To solve these problems, we have employed another gene transfer vector, *i.e.* LPD-II, composed of anionic lipids instead of cationic lipids (9). In this case, DNA only interacts with protamine and Dox. We expect that the enhanced entrapment efficiency would be achieved. In the following study, we explored the potential of LPD-II nanoparticles for the treatment of MDR cancer.

LPD-II Nanoparticles Avoided P-gp-mediated Drug Efflux from NCI/ADR-RES Cells—The third strategy developed in the study is to use a carrier, which has the high entrapment efficiency of Dox to avoid P-gp-mediated drug efflux. Only the drug presenting in the cell membrane can be effluxed out of the cancer cell. The drug delivered by nanoparticles is internalized in the cytoplasm or the lysosome and not pumped out by P-gp. The amount of Dox loaded into the LPD-II nanoparticles was ~90% of the total Dox determined by Sepharose CL 2B column chromatography. TEM images of the PEGylated LPD-II nanoparticles are shown in Fig. 4*A*. These nanoparticles are well dispersed spheres with sizes ranging from 20 to 50 nm. As shown in the confocal micrographs in Fig. 4*B*, the resulting nanoparticles efficiently delivered Dox (*red*) and FITC-labeled siRNA (*green*) to the NCI/ADR-RES cells. Dox was located in the nuclei of the cells, and siRNA was found in the cytoplasm.

Dox and siRNA uptake was further compared among different nanoparticle formulations by using flow cytometry. As can be seen in Fig. 4 (*C* and *D*), both siRNA and Dox delivered by targeted nanoparticles were taken up by NCI/ADR-RES cells more efficiently than those delivered by nontargeted nanoparticles or free drug. The uptake of Dox in the targeted nanoparticles was further examined in another drug-resistant cell line, P388/ADR cells, which also overexpressed P-gp. We modified the nanoparticles with a tumor targeting peptide that contained the Asn-Gly-Arg motif, a ligand of CD13 overexpressed in malignant myeloid leukemia cells such as P388 (15, 16). We have previously used the same Asn-Gly-Arg peptide to target siRNA to CD13-expressing cancer cells (14). As shown in supplemental Fig. S4, targeted nanoparticles increased Dox uptake compared with free Dox in P388/ADR cells. Thus, targeted LPD-II nanoparticles showed potential to deliver both siRNA and Dox to drug-resistant tumor cells in a target-specific manner.

We further studied the cy5.5-siRNA (*green*) and Dox (*red*) uptake of NCI/ADR-RES tumor tissue in the tumor-bearing mice 4 h after intravenous injections using confocal microscopy. As shown in Fig. 4*E*, the intracellular fluorescence signals were hardly detected in the tumor tissues collected from mice treated with nontargeted nanoparticles or free drug. The targeted nanoparticles showed strong cytosolic delivery of cy5.5-siRNA and nuclear delivery of Dox in the tumor tissue. Part of Dox co-localized with siRNA (*yellow*) in the cytoplasm of the tumor cells. These results indicate that the targeted nanoparticles could efficiently deliver siRNA and Dox to the tumor tissue, and the intracellular delivery was dependent on the presence of the ligand on the nanoparticles.

c-Myc siRNA Delivered by LPD-II Nanoparticles Down-regulated Both c-Myc and MDR Expression and Showed Enhanced Dox Uptake in NCI/ADR-RES Tumor—The last strategy we presented in this study is to co-deliver Dox and a therapeutic siRNA to inhibit both the survival signaling and the pathways that trigger drug resistance in MDR cancer cells. c-Myc, a transcription factor overexpressed in many human cancer cells, appears to play an important role in the regulation of cell growth and may activate MDR-1 transcription through the binding of the E-box motif (CACGTG) localized in the *MDR1* gene promoter (−272 and −444) (29). Therefore, c-Myc was chosen as a therapeutic target in the following study. To address the activities of siRNA *in vivo*, the c-Myc level in the tumor was assessed by quantitative reverse transcription-PCR and Western blot analysis (Fig. 5). Both c-Myc mRNA and protein expressions of the NCI/ADR-RES tumor treated with c-Myc siRNA and Dox-containing targeted nanoparticles were significantly inhibited (Fig. 5). c-Myc expression in NCI/ADR-RES tumor was silenced by c-Myc siRNA delivered with targeted nanoparticles (~40% of untreated control), whereas the nontargeted nanoparticles and the control siRNA showed no effect.

To verify the regulatory effects of c-Myc on the expression of MDR transporters (13), the protein levels of MDR transporters were measured 72 h after transfection of the siRNA targeting c-Myc. As shown in Fig. 6*A*, the MDR expression was significantly decreased in NCI/ADR-RES cells transfected with c-Myc siRNA compared with those transfected with control siRNA. To address the MDR down-regulation *in vivo*, the MDR level in the tumor was detected by immunostaining (Fig. 6*C*). The MDR expression of the NCI/ADR-RES tumor treated with c-Myc siRNA and Dox-containing targeted nanoparticles was significantly inhibited (Fig. 6*C*). Nontargeted nanoparticles and the control siRNA showed no effect.

To elucidate whether the down-regulation of the c-Myc expression could reverse the drug resistance of NCI/ADR-RES cells, Dox uptake was further compared among cells transfected *in vitro* with the c-Myc and control siRNAs by using flow cytometry. As shown in Fig. 6*B*, free Dox uptake was significantly increased in NCI/ADR-RES cells transfected with c-Myc siRNA compared with those transfected with control siRNA. We further studied the Dox uptake of NCI/ADR-RES tumor tissue in the tumor-bearing mice 4 h after intravenous injections using confocal microscopy. Tumor-bearing mice were given two daily injections of c-Myc or control siRNA (1.2 mg/kg) formulated in the targeted nanoparticles. As shown in Fig. 6*D*, the targeted nanoparticles encapsulating Dox showed an increased cytosolic delivery of Dox on NCI/ADR-RES cells compared with free drugs. Free Dox uptake was higher in the tumor tissues collected from the mice treated with c-Myc siRNA than the mice treated with control siRNA. Furthermore, the formulated Dox uptake was also slightly higher in the tumor tissues from mice treated with c-Myc siRNA than in those treated with control siRNA. These results indicate that the uptakes of both free and formulated Dox were enhanced after treatment with c-Myc siRNA in the targeted nanoparticles. These studies suggest that the down-regulation of c-Myc expression could reverse the drug resistance of NCI/ADR-RES cells through the regulation of MDR transporter expression.

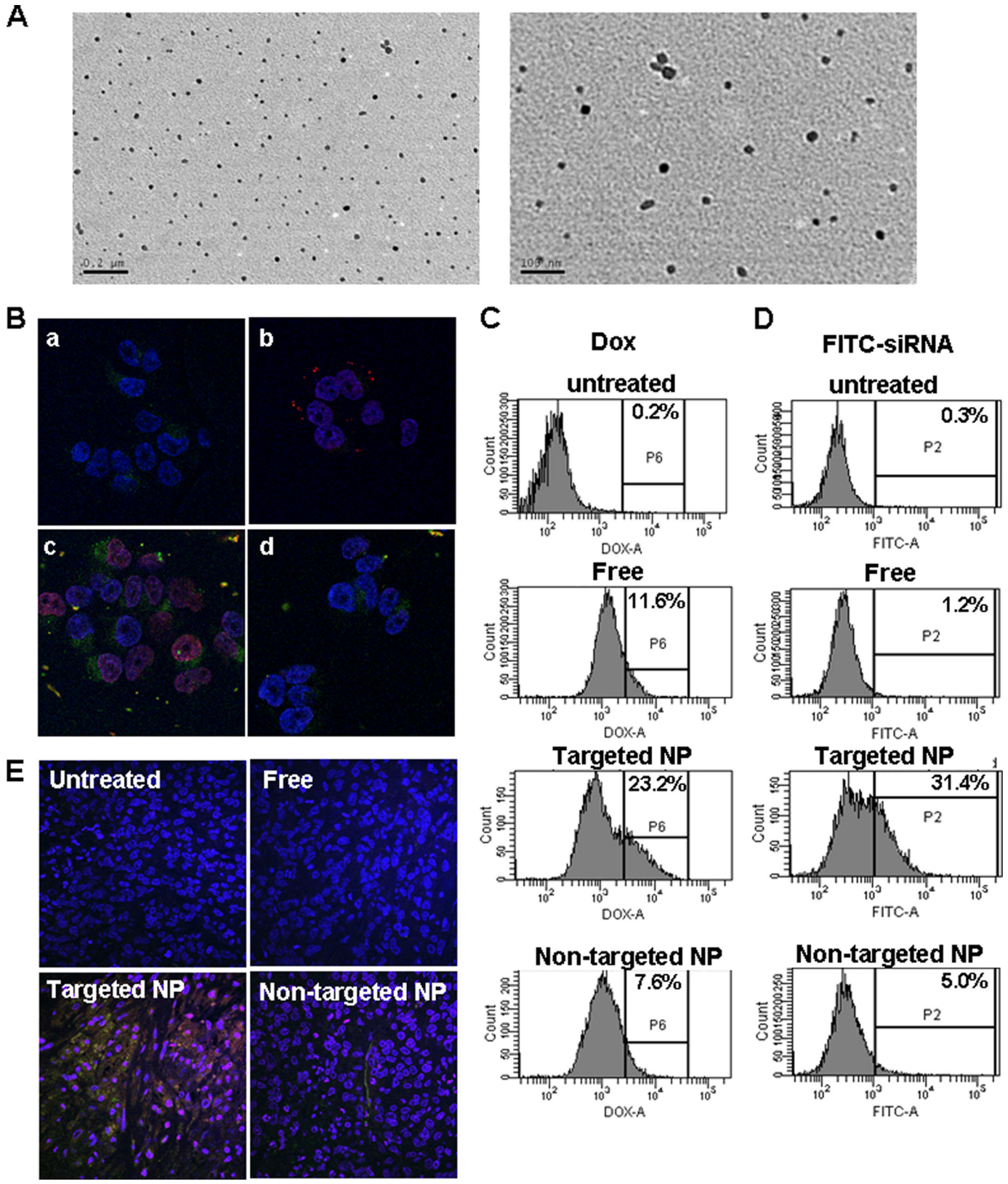

FIGURE 4. **Characterization of LPD-II nanoparticles.** *A*, TEM images of PEGylated LPD-II nanoparticles shown in two different magnifications. *B*, fluorescence photographs of NCI/ADR-RES cells after treatment with free siRNA (*green*) (*panel a*), free Dox (*red*) (*panel b*), siRNA and Dox in targeted nanoparticles (*panel c*), or nontargeted nanoparticles (*panel d*) for 1 h. *C* and *D*, quantitative measurement of Dox (*C*) and siRNA (*D*) uptake in NCI/ADR-RES cells by flow cytometry. The cells were treated with different formulations containing Dox or FITC-siRNA for 1 h and analyzed for fluorescence by flow cytometry. *E*, tumor uptake of siRNA and Dox in different formulations. Fluorescence signal of cy5.5-labeled siRNA and Dox in NCI/ADR-RES tumor was observed by confocal microscopy. The nuclei are *blue* (DAPI). *NP*, nanoparticles.

c-Myc siRNA and Dox Co-delivered by LPD-II Nanoparticles Showed Significant Therapeutic Effect in NCI/ADR-RES Tumor—To examine the apoptosis induced by the nanoparticles in the MDR tumors, we examined cellular apoptosis by using TUNEL staining (Fig. 7*A*). As shown in the figure, the number of TUNEL-positive cells increased after treatment of c-Myc siRNA and Dox co-delivered with the targeted nanoparticles. Intravenous injections of c-Myc siRNA and Dox in the nontargeted nanoparticles or the control siRNA and Dox in the targeted nanoparticles showed only a slight increase in TUNEL-positive cells. The level of the active caspase-3 was further detected by Western blot analysis (Fig. 7*B*). Activation of caspase-3 is a common mechanism triggered by factors that induce apoptosis (17). As shown in Fig. 7*B*, active caspase-3 in the NCI/ADR-RES tumor from mice treated with targeted nanoparticles containing c-Myc siRNA and Dox was significantly induced compared with those treated with other control formulations. There was a slight increase of the active caspase-3 in the tumors from mice treated with nontargeted nanoparticles or targeted nanoparticles containing Dox and control siRNA compared with the untreated mice. The results indicate that c-Myc siRNA and Dox formulated in the targeted nanoparticles could synergistically promote apoptosis in the NCI/ADR-RES tumor, and the cell killing effect was siRNA- and targeting ligand-dependent.

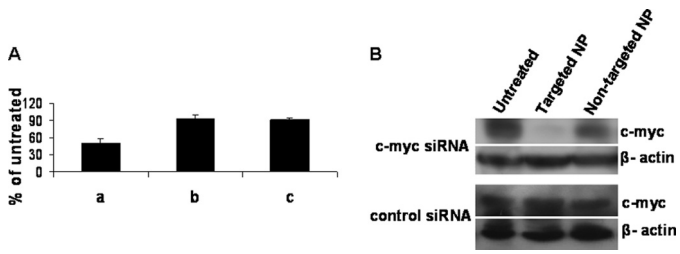

FIGURE 5. **c-Myc expression in NCI/ADR-RES xenograft tumor.** Shown is validation of c-Myc mRNA and protein expression in the NCI/ADR-RES xenograft tumor using real time PCR (*A*) and Western blot analysis (*B*) after treatment with different formulations. *Column a*, c-Myc siRNA and Dox co-formulated in targeted nanoparticles. *Column b*, c-Myc siRNA and Dox in non-targeted nanoparticles. *Column c*, control siRNA and Dox in targeted nanoparticles. *NP*, nanoparticles.

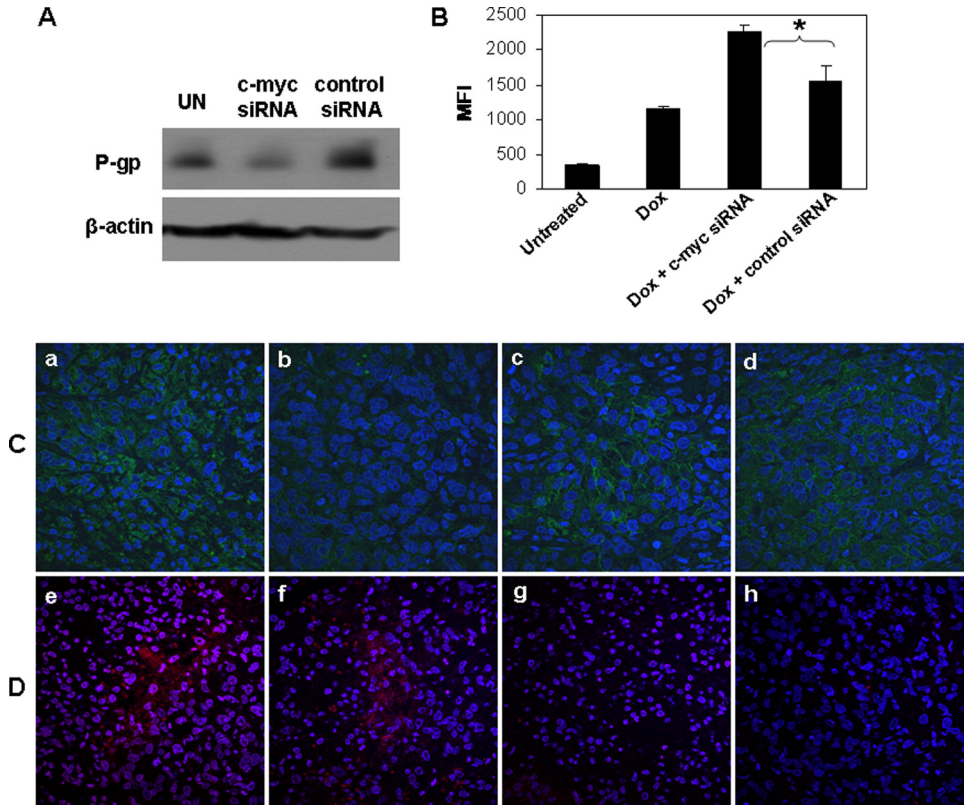

FIGURE 6. **MDR expression in NCI/ADR-RES xenograft tumor.** *A*, MDR expression in NCI/ADR-RES cells 72 h after transfection of siRNA with Lipofectamine *in vitro*. *B*, free Dox uptake in NCI/ADR-RES cells 72 h after transfection of siRNA with Lipofectamine. The cells were treated with free Dox for 30 min and analyzed for fluorescence by flow cytometry. The data are the mean values ± S.D.; $n = 3$. The *asterisk* indicates $p < 0.01$. *C*, MDR expression (*green*) in NCI/ADR-RES tumors 24 h after dosing of different formulations (two daily intravenous administrations of 1.2 mg/kg siRNA formulated in nanoparticles). *D*, tumor uptake of free Dox or Dox in the targeted nanoparticles 4 h after intravenous injection. Fluorescence signal of Dox (*red*) in NCI/ADR-RES tumor was observed by confocal microscopy. The nuclei are *blue* (DAPI). Tumor-bearing mice were given two daily injections of c-Myc or control siRNA (1.2 mg/kg) formulated in the targeted nanoparticles. Free Dox or Dox formulated in the targeted nanoparticles was intravenously injected into the tumor-bearing mice 24 h after the final treatment of siRNA. *Panel a*, untreated; *panel b*, c-Myc siRNA in targeted nanoparticles; *panel c*, c-Myc siRNA in nontargeted nanoparticles; *panel d*, control siRNA in targeted nanoparticles; *panel e*, intravenous administration of Dox in targeted nanoparticles 24 h after treatment of c-Myc siRNA; *panel f*, intravenous administration of Dox in targeted nanoparticles 24 h after treatment of control siRNA; *panel g*, intravenous administration of free Dox 24 h after treatment of c-Myc siRNA; *h*, intravenous administration of free Dox 24 h after treatment of control siRNA. *MFI*, mean fluorescence intensity.

To elucidate the synergistic effects of Dox and c-Myc siRNA, tumor growth inhibitory effects were examined *in vivo*. Three injections of control siRNA and Dox in the targeted nanoparticles showed a partial inhibition of tumor growth ($p < 0.05$ compared with the untreated control at day 18) (Fig. 7*C*). Other control groups treated with control siRNA formulated in the targeted nanoparticles without Dox or free Dox had no therapeutic effect. The results indicate that Dox formulated in the targeted nanoparticles showed an enhanced tumor inhibition effect.

Furthermore, three injections of c-Myc siRNA in the targeted nanoparticles failed to show the therapeutic effect (Fig. 7*D*). c-Myc siRNA and Dox in the nontargeted nanoparticles showed a partial inhibition of tumor growth ($p < 0.05$ at day 18) (Fig. 7*D*). A significant tumor growth inhibition was observed when mice were treated with Dox and c-Myc siRNA co-formulated in the targeted nanoparticles. Thus, targeted nanoparticles loaded with both Dox and c-Myc siRNA could overcome P-gp-mediated drug resistance.

Toxicity Study—In addition to efficacy, toxicity is another critical parameter of a suitable delivery vehicle for clinical use. Therefore,

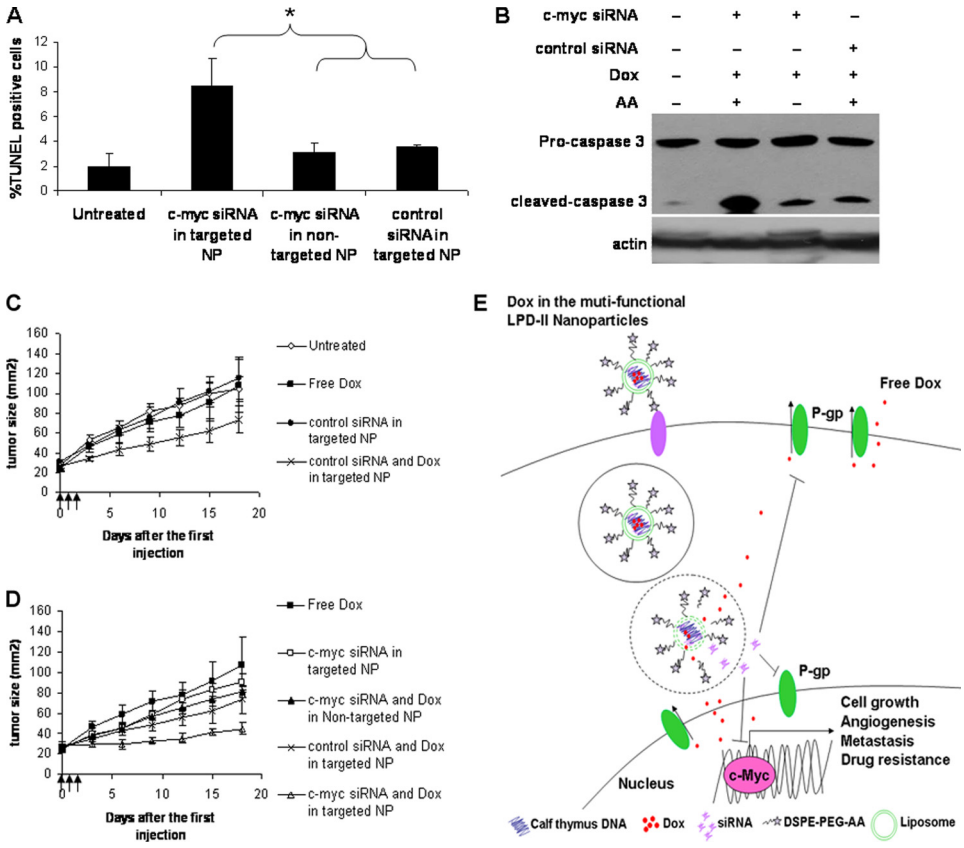

FIGURE 7. **Apoptosis induction and growth inhibition in NCI/ADR-RES xenograft tumor.** *A*, quantitative analysis of TUNEL positive staining in the tumors collected after two consecutive intravenous injections of siRNA and Dox in different formulations; $n = 3$. The *asterisk* indicates $p < 0.05$. *B*, caspase-3 activation in NCI/ADR-RES tumors 24 h after dosing of different formulations (two daily intravenous administrations of 1.2 mg/kg siRNA and 1.2 mg/kg Dox co-formulated in the nanoparticles). *C*, comparison of anti-tumor efficacy of free Dox and Dox delivered by targeted nanoparticles. *D*, comparison of anti-tumor efficacy of c-Myc siRNA and control siRNA co-formulated with Dox in different nanoparticles. The *arrows* indicate the intravenous administrations of siRNA (1.2 mg/kg) and Dox (1.2 mg/kg). The data are the mean values; $n = 5–7$. The standard deviations of the data points are not shown for clarity. *E*, schematic illustration of possible mechanisms to overcome drug resistance and achieve enhanced therapeutic effect in MDR cells using multifunctional LPD-II nanoparticles. *NP*, nanoparticles.

the proinflammatory cytokine (IL-6 and IL-12), hepatotoxicity maker (alanine aminotransferase and aspartate aminotransferase) levels, and the hematology parameters in the serum were examined for evaluation of toxicity induced by the nanoparticles in C57BL/6 mice (supplemental Table S1). siRNA and Dox formulated in the targeted LPD-II nanoparticles did not induce IL-6 and IL-12 significantly. Alanine aminotransferase and aspartate aminotransferase levels also remained the same as the untreated animals. Dox and siRNA formulated in the LPD-II targeted nanoparticles were very well tolerated with no significant changes in key hematology parameters. However, siRNA and Dox formulated in the targeted nanoparticles containing DSAA induced a significant production of IL-12. As shown in supplemental Table S1, the white blood cell count and platelet count were significantly reduced after treatment of siRNA and Dox in the targeted nanoparticles containing DSAA (LPD). Because treatment of siRNA and Dox in the LPD-II nanoparticles resulted in significantly enhanced drug uptake and an anti-cancer effect in MDR tumors without toxicity, we believe that LPD-II is a valuable lipid carrier for siRNA and drug delivery against MDR tumors.

DISCUSSION

The occurrence of drug resistance is an important obstacle of cancer therapy. Drug transporter proteins, such as those in the MDR family, are overexpressed in most drug-resistant cancer cell lines and recurrent tumors in cancer patients. Dox is known as a MDR substrate, and its reduced uptake and compromised therapeutic efficacy are related to MDR overexpression (18). In this study, our aim was to develop a multifunctional nanoparticle delivery system that can systemically deliver therapeutic siRNA and Dox into the drug-resistant tumors and achieve an enhanced therapeutic effect. We discuss several strategies in one single nanoparticle formulation to improve drug uptake in the MDR tumors. First, a guanidinium-containing cationic lipid, DSAA, was utilized to form LPD nanoparticles. We first demonstrated that DSAA induced ROS, inhibited the activity and expression of MDR transporters, and enhanced Dox uptake in NCI/ADR-RES cells (Fig. 1). However, cationic lipids without guanidinium groups did not cause these effects. Thus, the guanidinium group plays an important role in determining the activity of the lipids. It has been shown that guanidinium compounds generate ROS such as hydroxyl free radical (•OH) (19). The guanidium ion in the head group of DSAA may donate an electron to generate a superoxide-forming hydroxyl radical. Furthermore, it is known that ROS down-regulates MDR expression by activating c-Jun N-terminal kinase (JNK) and c-Jun in MDR cells (12, 20). ROS generated by DSAA may serve as a secondary messenger in the receptor tyrosine kinase signaling pathways and result in the down-regulation of MDR expression. In this study, DSAA served as both a formulation component to deliver siRNA and Dox into the MDR cells as well as a therapeutic agent that inhibited expression of MDR transporters and sensitized MDR cells to chemotherapy drugs.

Second, we co-delivered VEGF siRNA to target tumor vasculature, block angiogenesis, and disrupt local blood supply. We found an enhanced tumor uptake of free Dox and formulated Dox after the treatment with VEGF siRNA (Fig. 2). Furthermore, an enhanced growth inhibition of NCI/ADR-RES tumor was observed after co-delivery of VEGF siRNA and Dox in the targeted nanoparticles containing DSAA. VEGF siRNA alone or Dox alone in the targeted nanoparticles only achieved

a partial therapeutic effect. Several mechanisms may be involved in the anti-cancer effect of anti-VEGF therapy. Anti-angiogenesis triggered by VEGF siRNA can kill the tumor cells and sensitize the cells to chemotherapy agents by blocking blood supply. Furthermore, anti-angiogenic therapy can improve drug penetration as shown in Fig. 2. It may be due to disruption or normalization of tumor vasculature, which results in reduced interstitial fluid pressure and enhanced drug permeability (21–23).

On the other hand, instead of using a cationic formulation lipid, we developed second generation LPD (LPD-II) nanoparticles that contain a DNA polycation condensed core coated with an anionic lipid membrane consisting of mainly DOPA. Our previous study suggested that when the cationic liposomes interacted with the negatively charged DNA-protamine complex, there was a substantial loss of Dox from the nanoparticle-associated DNA, and Dox encapsulation in the final LPD nanoparticles was significantly reduced (14). Compared with the LPD nanoparticles, the current LPD-II nanoparticles made with anionic lipids could carry more Dox in the formulation.

Third, as illustrated in Fig. 7*E*, another approach to overcome drug-resistant cancer is to use a drug delivery vehicle to deliver Dox and to avoid P-gp-mediated drug efflux. As shown in Fig. 4, targeted nanoparticles delivered more Dox to NCI/ADR-RES cells than nontargeted nanoparticles or free Dox. Dox entrapped in the targeted nanoparticles induced a significantly increased tumor uptake (Fig. 4) in the NCI/ADR-RES tumor model. An enhanced therapeutic effect was achieved by the Dox formulated in the targeted nanoparticle (Fig. 7). The targeted nanoparticles may avoid P-gp-mediated drug efflux by using ligand-dependent internalization. The internalized drugs that cannot "see" the efflux transporter are not pumped out of the cells. Furthermore, the entrapped Dox may be maintained for a prolonged period of time in the circulation after intravenous administration and taken up more in the tumor tissue compared with the free Dox. The targeted nanoparticles that selectively deliver Dox to tumor cells can enhance both the therapeutic efficacy and the safety of the therapeutic agents.

The last strategy is to silence the MDR expression by siRNA. Instead of silencing the MDR itself, we chose to silence c-Myc for two reasons. The first is that c-Myc has been implicated to positively control MDR expression (24–26). Silencing c-Myc may result in the down-regulation of MDR, which appears to be expressed on plasma membrane and nuclear envelope (27, 28). The second is that c-Myc is a well known oncogene, the silencing of which may bring about a direct anticancer effect. In this study, we demonstrated that c-Myc siRNA delivered by targeted nanoparticles significantly down-regulated both c-Myc and MDR expressions in NCI/ADR-RES tumor, caused enhanced Dox uptake, and sensitized drug-resistant tumor cells to the co-delivered Dox (Figs. 5 and 6). c-Myc, a transcription factor overexpressed in many human cancer cells, may activate MDR-1 transcription through the binding of the E-box motif (CACGTG) localized in the *MDR1* gene promoter (−272 and −444) (29). Therefore, inhibition of c-Myc expression by siRNA results in the down-regulation of the MDR expression. This strategy is schematically illustrated in Fig. 7*E*.

TABLE 1

Comparison of two nanoparticle formulations delivering siRNA and Dox to overcome drug resistance for cancer therapy

Property	I. LPD nanoparticles containing a guanidinium lipid	II. LPDII nanoparticles containing an anionic lipid
Therapeutic cargos	DSAA, VEGF siRNA and Dox	c-myc siRNA and Dox
The Mechanism of overcoming MDR	1. a delivery vehicle to avoid P-gp mediated drug efflux. 2. a guanidinium-containing cationic lipid, DSAA to inhibit MDR transporters and enhance Dox uptake.	1. a delivery vehicle to avoid P-gp mediated drug efflux. 2. c-myc siRNA to downregulate MDR expression and increase Dox uptake.
Zeta potential (mV)	35 ± 8	-19.4 ± 1.1
Particle size (nm)	135 ± 7	62.7 ± 13.3
Entrapment efficiency of Dox	Low (about 10%)	High (about 90%)
Transfection efficiency of siRNA *in vitro*	High	Low
Toxicity	Serum IL-12 ↑; WBC↓; PLT ↓.	None
Apoptosis induction (% TUNEL positive cells)	About 8 %	About 8%
Tumor growth inhibition	Significant compared with free Dox, Dox or siRNA alone in the targeted nanoparticles.	Significant compared with free Dox, Dox or siRNA alone in the targeted nanoparticles.

We have developed two different but novel nanoparticles to overcome drug resistance for cancer therapy. The comparisons between two nanoparticle formulations are listed in Table 1. Both multifunctional nanoparticle formulations can deliver Dox and siRNA to MDR tumor simultaneously. The same amount of siRNA and Dox delivered by targeted LPD and LPD-II showed similar apoptosis inductions and therapeutic efficacies in NCI/ADR tumors. However, based on the toxicity study, LPD nanoparticles containing DSAA induced more toxicity compared with LPD-II nanoparticles. The mechanism of immunotoxicity induced by LPD nanoparticles containing DSAA may be mediated through the interaction between the cationic lipid and immune cells (30). In conclusion, LPD-II nanoparticles with a higher entrapment efficiency of Dox and a lower toxicity profile may show a larger therapeutic window and potential clinical application for cancer therapy than the LPD nanoparticles. To our knowledge, this is the first parallel preclinical study of systemic co-delivery of therapeutic siRNA and a chemotherapy drug to a drug-resistant tumor using two different multifunctional gene delivery systems.

Acknowledgment—We thank the Michael Hooker Microscopy Facility at University of North Carolina for the microscopy images. Srinivas Ramishetti assisted in preparing the manuscript.

REFERENCES

1. Shah, N., Chaudhari, K., Dantuluri, P., Murthy, R. S., and Das, S. (2009) *J. Drug Target* **17,** 533–542
2. Xu, D. H., Gao, J. Q., and Liang, W. Q. (2008) *Pharmazie* **63,** 646–649
3. Goren, D., Horowitz, A. T., Tzemach, D., Tarshish, M., Zalipsky, S., and Gabizon, A. (2000) *Clin. Cancer Res.* **6,** 1949–1957
4. Devi, G. R. (2006) *Cancer Gene Ther.* **13,** 819–829
5. Shen, Y. (2008) *IDrugs* **11,** 572–578
6. Chen, Y., Sen, J., Bathula, S. R., Yang, Q., Fittipaldi, R., and Huang, L. (2009) *Mol. Pharm.* **6,** 696–705
7. Holló, Z., Homolya, L., Hegedüs, T., and Sarkadi, B. (1996) *FEBS Lett.* **383,** 99–104
8. Cui, Z., Han, S. J., Vangasseri, D. P., and Huang, L. (2005) *Mol. Pharmacol.* **2,** 22–28
9. Lee, R. J., and Huang, L. (1996) *J. Biol. Chem.* **271,** 8481–8487
10. Song, E., Zhu, P., Lee, S. K., Chowdhury, D., Kussman, S., Dykxhoorn, D. M., Feng, Y., Palliser, D., Weiner, D. B., Shankar, P., Marasco, W. A., and

Lieberman, J. (2005) *Nat. Biotechnol.* **23,** 709–717
11. Hiramatsu, M. (2003) *Mol. Cell Biochem.* **244,** 57–62
12. Cai, Y., Lu, J., Miao, Z., Lin, L., and Ding, J. (2007) *Cancer Biol. Ther.* **6,** 1794–1799
13. Almubarak, M., Newton, M., and Altaha, R. (2008) *J. Oncol.* 2008, 942618
14. Chen, Y., Wu, J. J., and Huang, L. (2010) *Mol. Ther.* **18,** 828–834
15. Tsuruo, T., Naganuma, K., Iida, H., Yamori, T., Tsukagoshi, S., and Sakurai, Y. (1981) *J. Antibiot.* **34,** 1206–1209
16. Mishima, Y., Matsumoto-Mishima, Y., Terui, Y., Katsuyama, M., Yamada, M., Mori, M., Ishizaka, Y., Ikeda, K., Watanabe, J., Mizunuma, N., Hayasawa, H., and Hatake, K. (2002) *J. Natl. Cancer Inst.* **94,** 1020–1028
17. Jänicke, R. U., Ng, P., Sprengart, M. L., and Porter, A. G. (1998) *J. Biol. Chem.* **273,** 15540–15545
18. Puhlmann, U., Ziemann, C., Ruedell, G., Vorwerk, H., Schaefer, D., Langebrake, C., Schuermann, P., Creutzig, U., and Reinhardt, D. (2005) *J. Pharmacol. Exp. Ther.* **312,** 346–354
19. Mori, A. (1987) *Pavlov. J. Biol. Sci.* **22,** 85–94
20. Wartenberg, M., Ling, F. C., Schallenberg, M., Bäumer, A. T., Petrat, K., Hescheler, J., and Sauer, H. (2001) *J. Biol. Chem.* **276,** 17420–17428
21. Tong, R. T., Boucher, Y., Kozin, S. V., Winkler, F., Hicklin, D. J., and Jain, R. K. (2004) *Cancer Res.* **64,** 3731–3736
22. Vlahovic, G., Ponce, A. M., Rabbani, Z., Salahuddin, F. K., Zgonjanin, L., Spasojevic, I., Vujaskovic, Z., and Dewhirst, M. W. (2007) *Br. J. Cancer* **97,** 735–740
23. Nakahara, T., Norberg, S. M., Shalinsky, D. R., Hu-Lowe, D. D., and McDonald, D. M. (2006) *Cancer Res.* **66,** 1434–1445
24. Nakamura, Y., Sato, H., and Motokura, T. (2006) *Int. J. Cancer* **118,** 2448–2454
25. He, Y., Zhang, J., and Yuan, Y. (2000) *Chin. Med. J.* **113,** 848–851
26. Banerjee, S., Ganapathi, R., Ghosh, L., and Yu, C. L. (1992) *Cell Mol. Biol.* **38,** 561–570
27. Calcabrini, A., Meschini, S., Stringaro, A., Cianfriglia, M., Arancia, G., and Molinari, A. (2000) *Histochem. J.* **32,** 599–606
28. Gervasoni, J. E., Jr., Fields, S. Z., Krishna, S., Baker, M. A., Rosado, M., Thuraisamy, K., Hindenburg, A. A., and Taub, R. N. (1991) *Cancer Res.* **51,** 4955–4963
29. Grandjean-Forestier, F., Stenger, C., Robert, J., Verdier, M., and Ratinaud, M. H. (2009) *ABC Transporters and Multidrug Resistance*, pp. 17–26, Wiley-Liss, New York
30. Yan, W., Chen, W., and Huang, L. (2007) *Mol. Immunol.* **44,** 3672–3681